Bulletin of Electrical Engineering and Informatics
Vol. 9, No. 2, April 2020, pp. 452~465
ISSN: 2302-9285, DOI: 10.11591/eei.v9i2.1682

Induction motor harmonic reduction using space vector modulation algorithm

Yassine Zahraoui, Mohamed Akherraz, Chaymae Fahassa, Sara Elbadaoui
Department of Electrical Engineering, Mohamed 5 University, Mohammadia School of Engineering, Morocco

Article Info

Article history:

Received Jul 18, 2019
Revised Sep 26, 2019
Accepted Nov 15, 2019

Keywords:

Harmonic reduction
Induction motor
Integral backstepping control
Space vector modulation
Speed sensorless

ABSTRACT

The vector control was proposed as an alternative to the scalar control for AC machines control. It provides high operation performance in steady state and transient operation. However, the variable switching frequency of vector control causes high flux and torque ripples which lead to an acoustical noise and degrade the performance of the control scheme. The insertion of the space vector modulation was a very useful solution to reduce the high ripples level inspite of its complexity. Numerical simulation results obtained in MATLAB/Simulink show the good dynamic performance of the proposed vector control technique and the effectiveness of the proposed sensorless strategy in the presence of the sudden load torque basing on the integral backstepping approach capabilities on instant perturbation rejection.

Corresponding Author:

Yassine Zahraoui,
Department of Electrical Engineering,
Mohamed 5 University, Mohammadia School of Engineering,
Street Ibn Sina, B.P 675, Agdal, Morocco.
Email: zahraoui.yassin@gmail.com

1. INTRODUCTION

Nowadays, the AC machines have replaced the DC machines in industrial applications because of their advantages, such as, the reliability and the lack of commutator and brushes which make them able to work under unfriendly conditions. The most popular AC machines are the induction motors (IM) and the permanent magnet synchronous motors. They are used in various industrial applications, electric vehicles, tools and drives etc. The squirrel cage induction motor in particular, is widely used due to its reduced cost and lower maintenance requirement [1].

In the early decades, the induction motors have been operated directly from the grid under a fixed frequency-speed. Later, with the development of modern semiconductor devices and power electronic converters, these machines had become able to operate with adjustable frequency-speed by supplying them through a power converter like the voltage source inverter. The employment of the variable speed motor drive in open loop may offer a satisfied performance at steady state without need of speed regulation for simple applications [2]. But, in cases where the drive requires fast dynamic response and accurate speed, the open loop control becomes unsatisfactory. Therefore, it is necessary to operate the motor in a closed loop mode. Several techniques have been proposed for this purpose. They are classified mainly into scalar and vector controls [3].

The vector control, which is known also by the field-oriented control (FOC), was developed to overcome the limitation of the scalar control. It was presented in the 1970s by Hasse [4] and Blaschke [5] to provide an independent control of torque and flux in similar way to the separate excitation DC machine. The vector representation of the motor quantities makes it valid to work in both steady and dynamic

conditions, this achieves a good transient response. In the control algorithm of FOC based on the transformation to the synchronous frame, all quantities will appear as DC quantities.

However, the standard FOC method suffers from high phase current, line voltage and torque ripples. Many modified FOC schemes have been proposed in order to reduce ripples. The insertion of the space vector modulation (SVM) was a very useful solution [6]. This method, known by SVM-FOC, reduces the high ripples level in spite of its complexity. SVM-FOC algorithm uses linear PI torque and flux controllers to generate the reference control voltages [7].

The initial mathematical model based on conventional analytic methods usually contains approximate hypothesis and unmodeled dynamics. Moreover, it may be affected also by the variation in parameters due to environment conditions and the external disturbance during operating. Consequently, the use of linear methods such the PI controllers cannot achieve high promising performance. The nonlinear controllers can offer several advantages compared to linear control schemes. Among the interest researches in the field of nonlinear control techniques are the sliding mode control (SMC) [8] and the backstepping control (BSC) with integral action [9].

Moreover, the sensorless control is another major issue in control domain. The developed control schemes using advanced strategies such as the SVM and nonlinear techniques require an accurate speed and flux measurement or estimation for closed loop control design [10]. The use of sensors has several downsides like high cost, fragility and low reliability. Furthermore, the physical environment sometimes, does not allow to use sensors. Due to the multiple variables and nonlinearity of induction motor dynamics, the estimation of the rotor speed and flux without the measurement is still very challenging subject. Various sensorless approaches have been proposed in the literature [11].

2. INDOCTION MOTOR MODELING

Developing new control laws of observation and optimization for the IM naturally imposes not to neglect the modelling aspect of this machine. The modelling of AC machines is based mainly on the work of G. Kron, who gave birth to the concept of generalized machine [12]. Park's model is a special case of this concept. It is often used for the synthesis of control laws and estimators. Described by a non linear algebra-differential system, Park's model reflects the dynamic behaviour of the electrical and electromagnetic modes of the asynchronous machine. It admits several classes of state representations. These model classes depend directly on the control objectives (torque, speed, position), the nature of the power source of the work repository and the choice of state vector components (flux or currents, stator or rotor).The IM drive can be described by the following state equations in the rotating field reference frame.

$$\begin{aligned} \dot{X} &= \mathbf{A}X + \mathbf{B}U \\ Y &= \mathbf{C}X \end{aligned} \tag{1}$$

Where X, U and Y are the state vector, the input vector and the output vector respectively. With:

$$X = \left[i_{ds} i_{qs} \phi_{dr} \phi_{qr}\right]^T ; U = \left[u_{ds} u_{qs}\right]^T ; Y = \left[i_{ds} i_{qs}\right]^T$$

$$\mathbf{A} = \begin{bmatrix} -a_1 & \omega_s & a_2 & a_3.\omega_r \\ -\omega_s & -a_1 & -a_3.\omega_r & a_2 \\ a_4 & 0 & -a_5 & \omega_r \\ 0 & a_4 & -\omega_r & -a_5 \end{bmatrix} ; \mathbf{B} = \begin{bmatrix} \frac{1}{\sigma L_s} & 0 \\ 0 & \frac{1}{\sigma L_s} \\ 0 & 0 \\ 0 & 0 \end{bmatrix} ; \mathbf{C} = \begin{bmatrix} 1 & 0 & 0 & 0 \\ 0 & 1 & 0 & 0 \end{bmatrix}$$

$$\text{And } a_1 = \frac{R_s}{\sigma L_s} + \frac{R_r L_m^2}{\sigma L_s L_r} ; a_2 = \frac{L_m}{\sigma L_s L_r T_r} ; a_3 = \frac{L_m}{\sigma L_s L_r} ; a_4 = \frac{L_m}{T_r} ; a_5 = \frac{1}{T_r} ; T_r = \frac{L_r}{R_r}$$

3. DIRECT FIELD ORIENTED CONTROL BASED BACKSTEPPING APPROACH

3.1. Main objective of vector control

The main objective of the field-oriented control is to set a simple model of the IM drive in which the flux component and the current magnitude are separated. For a DC machine, the field inductor and the induced current are naturally decoupled and orthogonal. In the case of an IM, it is difficult to distinguish the torque-producing current and the flux-producing current, which are strongly coupled [13, 14].The idea of the oriented field is to choose a two-phase rotating axis system (d, q) mounted on the rotor, stator or air gap, allowing decoupling the torque and the flux. Rotor flux orientation control

is the most widely used because it eliminates the influence of rotor and stator leakage reactance and gives better results than methods based on stator flux or gap orientation [11]. The condition of this alignment is expressed by the following relation:

$$\phi_{dr} = \phi_r \;\; ; \;\; \phi_{qr} = 0$$

The direct version of the vector control requires a good knowledge of the module and the phase of the flux. The first idea is to access the flux from sensors located in the air gap of the machine. However, the introduction of these sensors causes an increase in volume and weakening of the machine [15]. In addition, these sensors are sensitive to mechanical shocks and temperature variations. Instead, measured quantities such as stator voltages and currents can be used to estimate or observe the rotor flux. In this type of control, the norm of the flux and its position used for the transformation of the coordinates are determined as follows:

$$\phi_r = \sqrt{(\phi_{\alpha r}^2 + \phi_{\beta r}^2)} \quad (2)$$

$$\theta_s = \text{Arctg}\left(\frac{\phi_{\beta r}}{\phi_{\alpha r}}\right) \quad (3)$$

With:

$$\phi_{\alpha r} = \frac{L_r}{L_m}\left(\int (V_{\alpha s} - R_s i_{\alpha s})dt - \sigma L_s i_{\alpha s}\right)$$

$$\phi_{\beta r} = \frac{L_r}{L_m}\left(\int \left(V_{\beta s} - R_s i_{\beta s}\right)dt - \sigma L_s i_{\beta s}\right)$$

Note that the essential problem of the vector control is to determine the position and the norm of the rotor flux.

3.2. Backkstepping approach applied to direct vector control of IM drive

The backstepping approach is a technique of systematic and recursive synthesis intended for the class of nonlinear systems, the basic idea behind backstepping is to recursively select some appropriate state functions as virtual command inputs for first-order subsystems of the global system. In each step, an extended Lyapunov function is associated to ensure the stability of the entire system [16].

Step 1:

In this step, the speed and the rotor flux are regulation components; we define the regulation errors e_1 and e_2 by:

$$e_1 = \Omega^* - \Omega$$
$$e_2 = \phi_{dr}^* - \phi_{dr}$$

Since the objective requires that both errors converge to zero, we choose i_{qs} and i_{ds} as virtual commands for the system, for this, we consider the candidate Lyapunov function:

$$V_1 = \frac{1}{2}[e_1^2 + e_2^2] \quad (4)$$

Its derivative is:

$$\dot{V}_1 = -\mathbf{k_1} e_1^2 - k_2 e_2^2 + e_1\left[\mathbf{k_1} e_1 + \dot{\Omega}^* - \mu\phi_{dr} i_{qs} + \frac{T_L}{J}\frac{f}{J}\Omega\right] + e_2\left[\mathbf{k_2} e_2 + \dot{\phi}_{dr}^* + \frac{1}{T_r}\phi_{dr} - \frac{L_m}{T_r} i_{ds}\right] \quad (5)$$

Where $\mathbf{k_1}$ and $\mathbf{k_2}$ are positive constants.

So that the derivative of the Lyapunov function is negative, the virtual commands representing the stabilizing functions can be chosen as:

$$i_{qs}^* = \frac{1}{\mu\phi_{dr}}[\mathbf{k_1} e_1 + \dot{\Omega}^* + \frac{T_L}{J} + \frac{f}{J}\Omega] \quad (6)$$

$$i_{ds}^{*} = \frac{T_r}{L_m}[\mathbf{k_2}e_2 + \dot{\phi}_{dr}^{*} + \frac{1}{T_r}\phi_{dr}] \quad (7)$$

We then obtain:

$$\dot{V}_1 = -\mathbf{k_1}e_1^2 - \mathbf{k_2}e_2^2 \leq 0$$

The virtual commands in (6) and (7) are chosen to satisfy the pursuit objectives and are also considered as references for the next step.

Step 2:

Now the currents i_{qs} and i_{ds} are the new control components considered as virtual commands of this step, we define the regulation errors e_3 and e_4:

$$e_3 = i_{qs}^{*} - i_{qs} \;;\; e_4 = i_{ds}^{*} - i_{ds}$$

Therefore, error dynamics e_3 and e_4 can be expressed by:

$$\dot{e_3} = \dot{\imath}_{qs}^{*} - \psi_1 - \frac{1}{\sigma L_s}v_{qs}$$

$$\dot{e_4} = \dot{\imath}_{ds}^{*} - \psi_2 - \frac{1}{\sigma L_s}v_{ds}$$

Where:

$$\psi_1 = -\gamma i_{qs} - \mu\Omega\phi_{dr} - p\Omega i_{ds} - \frac{L_m}{T_r}\frac{i_{ds}i_{qs}}{\phi_{dr}} \quad (8)$$

$$\psi_2 = -\gamma i_{ds} - \frac{\mu}{T_r}\phi_{dr} + p\Omega i_{qs} + \frac{L_m}{T_r}\frac{i_{ds}^2}{\phi_{dr}} \quad (9)$$

Consider the following Lyapunov candidate function:

$$V_2 = \frac{1}{2}[e_1^2 + e_2^2 + e_3^2 + e_4^2] \quad (10)$$

Its time derivative is given by:

$$\dot{V}_2 = -\mathbf{k_1}e_1^2 - \mathbf{k_2}e_2^2 - \mathbf{k_3}e_3^2 - \mathbf{k_4}e_4^2 + e_3\left[\mathbf{k_3}e_3 + \dot{\imath}_{qs}^{*} - \psi_1 - \frac{1}{\sigma L_s}v_{qs}\right] + e_4[\mathbf{k_4}e_4 + \dot{\imath}_{ds}^{*} - \psi_2 - \frac{1}{\sigma L_s}v_{ds}]$$

Where $\mathbf{k_3}$ and $\mathbf{k_4}$ are positive constants. Then, the following control laws are deduced:

$$v_{qs}^{*} = \sigma L_s[\mathbf{k_3}e_3 + \dot{\imath}_{qs}^{*} - \psi_1] \quad (11)$$

$$v_{ds}^{*} = \sigma L_s[\mathbf{k_4}e_4 + \dot{\imath}_{ds}^{*} - \psi_2] \quad (12)$$

Which makes the derivative of the extended Lyapunov function $\dot{V}_2$ negative:

$$\dot{V}_2 = -\mathbf{k_1}e_1^2 - \mathbf{k_2}e_2^2 - \mathbf{k_3}e_3^2 - \mathbf{k_4}e_4^2 \leq 0$$

Proposition 1:*Consider the model of the IM (1). If the speed and flux controllers synthesized by the backstepping method are given by (11) and (12) respectively, then these commands are such that the flux and speed converge asymptotically to their desired values.*

3.3. Backstepping approach with integral action for robust control

It is clear that the structure of the controller generated by the classic version of the backstepping is composed of a proportional action, to which is added a derivate action on the error. Such a structure makes the system sensitive to measurement noises [17]. The absence of the integrator action leads to the appearance of a non-zero constant static error. The solution of this problem is the design of a new version of the backstepping with an integral action. Integrators should be integrated into the machine model and apply the conventional backstepping method to this new model. The integral action will be automatically transferred from the model to the control law [18].

Speed tracking error is defined by:

$$z_1 = e_1 + \boldsymbol{\delta_1} \int e_1 dt$$

With $\boldsymbol{\delta_1}$ is a positive constant and $\delta_1 \int e_1 dt$ is the integral action added to the backstepping control to ensure convergence of the speed tracking error to zero.
Consider the candidate function of Lyapunov and its derivative given by:

$$V_1 = \frac{1}{2} z_1^2 \tag{13}$$

$$\dot{V_1} = -\mathbf{k_1} z_1^2 + z_1 \left[\mathbf{k_1} z_1 + \dot{\Omega^*} - \mu \phi_{dr} i_{qs} + \frac{T_L}{J} + \frac{f}{J} \Omega + \boldsymbol{\delta_1} e_1 \right]$$

According to the backstepping method and in order to ensure the speed tracking stability, the virtual control i_{qs}^* is given by the following equation:

$$i_{qs}^* = \frac{1}{\mu \phi_{dr}} [\mathbf{k_1} z_1 + \dot{\Omega^*} + \frac{T_L}{J} + \boldsymbol{\delta_1} e_1] \tag{14}$$

We then get:

$$\dot{V_1} = -\mathbf{k_1} z_1^2 \leq 0$$

The state i_{qs}^* is then used as an intermediate command to ensure stability. The time derivative of z_3 is given by:

$$\dot{z_3} = \dot{\imath_{qs}^*} - \dot{\imath_{qs}}$$

Consider the extended Lyapunov candidate function and its derivative given by:

$$V_2 = V_1 + \frac{1}{2} z_3^2 \tag{15}$$

$$\dot{V_2} = -\mathbf{k_1} z_1^2 - \mathbf{k_3} z_3^2 + z_2 \left[\mathbf{k_3} z_3 + \dot{\imath_{qs}^*} - \psi_1 - \frac{1}{\sigma L_s} v_{qs} \right]$$

By choosing the control law V_{qs}^* as:

$$V_{qs}^* = \sigma L_s \left[\mathbf{k_3} z_3 + \dot{\imath_{qs}^*} - \psi_1 \right] \tag{16}$$

We find that:

$$\dot{V_2} = -\mathbf{k_1} z_1^2 - \mathbf{k_3} z_3^2 \leq 0 \tag{17}$$

4. SPACE VECTOR MODULATION ALGORITHM FOR RIPPLES REDUCTION

In this FOC strategy, the pulse width modulation (PWM) is replaced by the space vector modulation (SVM) for the purpose of voltage vector selection. This control schemes can preserve a constant switching frequency, consequently it reduces the high torque and phase current ripples which is the main drawback of the conventional FOC. SVM was first presented in the second half of the 1980s as an alternative strategy to the basic Pulse Width Modulator (PWM). Since then, a lot of work has been done on its theory and implementation. SVM bases on the space vector representation of the voltage inverter output. It has several advantages such as minimizing ripple and Total Harmonic Distortion (THD) and switching losses [19].

SVM is different from the conventional pulse width modulation (PWM). It relies on the space vector representation of the inverter output. There are no separate modulators for each phase. The reference voltages are given by space voltage vector (i.e. voltage vector components in the complex plan). The principle of SVM is the prediction of inverter voltage vector by the projection of the reference vector V_s between adjacent vectors corresponding to two non-zero switching states [20]. For two-levels inverter, the switching vectors diagram forms a hexagon divided into six sectors, each one is expanded by 60° as shown in Figure 1.

The application time for each vector can be obtained by vector calculations and the rest of the time period will be spent by applying the null vector. When the reference voltage is in sector 1 as shown in Figure 2, the reference voltage can be synthesized by using the vectors V_1, V_2, and V_0(zero vector) [21].

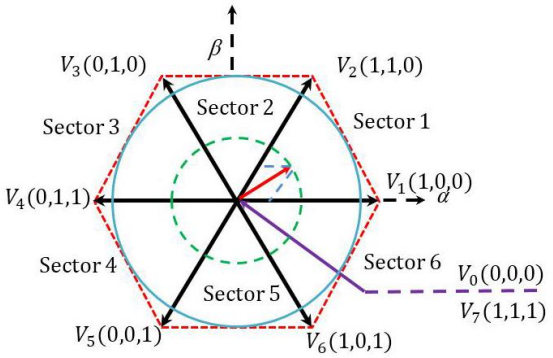

Figure 1. Diagram of voltage space vector

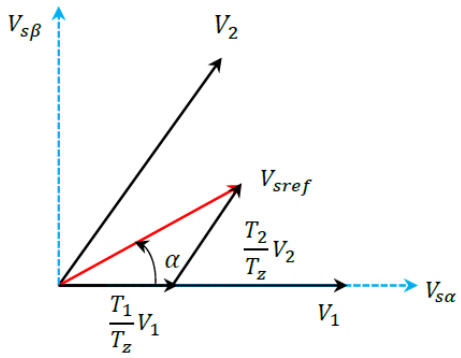

Figure 2. Reference vector as a combination of adjacent vectors at sector 1

The volt-second principle for sector 1 can be expressed by:

$$V_s^* T_z = V_1 T_1 + V_2 T_2 + V_0 T_0 \quad (18)$$

$$T_z = T_1 + T_2 + T_0 \quad (19)$$

T_1, T_2 and $T_0$are the corresponding application times of the voltage vectors respectively. $T_z$is the sampling time. The determination of times $T_1$and T_2corresponding to voltage vectors are obtained by simple projections:

$$T_1 = \frac{T_z}{2V_{dc}}\left(\sqrt{6}V_{s\beta}^* - \sqrt{2}V_{s\alpha}^*\right) \quad (20)$$

$$T_2 = \frac{\sqrt{2}T_z}{V_{dc}} V_{s\alpha}^* \quad (21)$$

With V_{dc} is the DC bus voltage.The calculation of switching times (duty cycles) is expressed as follows [22, 23]. as shown in Figure 3 andsummarizes switching times (output) for each sector as shown in Table 1.

$$T_{a_{on}} = \frac{T_z - T_1 - T_2}{2} \quad (22)$$

$$T_{b_{on}} = T_{a_{on}} + T_1 \quad (23)$$

$$T_{c_{on}} = T_{b_{on}} + T_2 \quad (24)$$

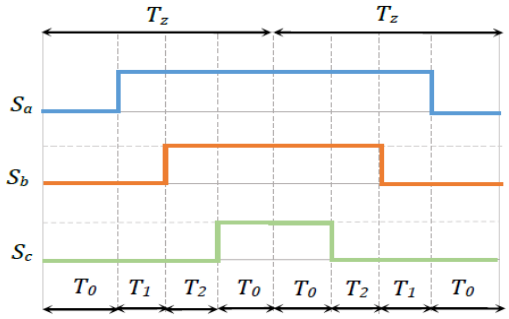

Figure 3. Switching times of sector 1

Table 1. Switching times for each sector

Sector	1	2	3	4	5	6
S_a	$T_{b_{on}}$	$T_{a_{on}}$	$T_{a_{on}}$	$T_{c_{on}}$	$T_{b_{on}}$	$T_{c_{on}}$
S_b	$T_{a_{on}}$	$T_{c_{on}}$	$T_{b_{on}}$	$T_{b_{on}}$	$T_{c_{on}}$	$T_{a_{on}}$
S_c	$T_{c_{on}}$	$T_{b_{on}}$	$T_{c_{on}}$	$T_{a_{on}}$	$T_{a_{on}}$	$T_{b_{on}}$

5. ADAPTIVE FUZZY LUENBERGER OBSERVER FOR FLUX AND SPEED ESTIMATION

The Adaptive flux observer is a deterministic type of observers based on a deterministic model of the system. In this work, the adaptive Luenberger state observer (ALO) is used to estimate the flux components and rotor speed of the IM drive by including an adaptive mechanism based on the Lyapunov theory [24] and fuzzy regulation. In general, the equations of the ALO can be expressed as follow:

$$\begin{cases} \dot{\hat{X}} = A.\hat{X} + B.U + L.(Y - \hat{Y}) \\ \hat{Y} = C.\hat{X} \end{cases} \quad (25)$$

The symbol ˆ denotes the estimated value and L is the observer gain matrix. The mechanism of adaptation speed is deduced by Lyapunov theory. The estimation error of the stator current and rotor flux, which is the difference between the observer and the model of the motor [25], is given by:

$$\dot{e} = (A - L.C).e + \Delta A.\hat{X} \quad (26)$$

Where $e = X - \hat{X}$ $\quad \Delta A = A - \hat{A} = \begin{bmatrix} 0 & 0 & 0 & K.\Delta\omega_r \\ 0 & 0 & -K.\Delta\omega_r & 0 \\ 0 & 0 & 0 & -\Delta\omega_r \\ 0 & 0 & \Delta\omega_r & 0 \end{bmatrix}$

We consider the following Lyapunov function:

$$V = e^t.e + \frac{(\Delta\omega_r)^2}{\lambda} \quad (27)$$

Where λ is a positive coefficient, its derivative is given as:

$$\dot{V} = e^t[(A - LC)^t + (A - LC)]e - 2K\Delta\omega_r.(e_{i\alpha s}\widehat{\phi_{\beta r}} - e_{i\beta s}\widehat{\phi_{\alpha r}})$$

With $\widehat{\omega_r}$ is the estimated rotor speed. The adaptation law for the estimation of the rotor speed can be deduced by the equality between the second and third terms of (9):

$$\widehat{\omega_r} = \int \lambda.K.\left(e_{i\alpha s}\widehat{\phi_{\beta r}} - e_{i\beta s}\widehat{\phi_{\alpha r}}\right).dt \quad (28)$$

The feedback gain matrix L is chosen to ensure the fast and robust dynamic performance of the closed loop observer.

$$L = \begin{bmatrix} l_1 & -l_2 \\ l_2 & l_1 \\ l_3 & -l_4 \\ l_4 & l_3 \end{bmatrix} \quad (29)$$

With l_1, l_2, l_3 and l_4 are given by:

$$l_1 = (k_1 - 1).(\gamma + \frac{1}{T_r}) \quad ; \quad l_2 = -(k_1 - 1).\widehat{\omega_r} \quad ; \quad l_3 = \frac{(k_1^2 - 1)}{K}.\left(\gamma - K.\frac{L_m}{T_r}\right) + \frac{(k_1 - 1)}{K}.(\gamma + \frac{1}{T_r}) \quad ;$$
$$l_4 = -\frac{(k_1 - 1)}{K}.\widehat{\omega_r}$$

k_1 is a positive coefficient obtained by pole placement approach; a wise choice was made for its value in order to guarantee a fast response. Fuzzy logic control (FLC) in adaptation mechanism replaces conventional control and it gives robust performance against parameter variation and machine saturation [26, 27]. Figure 4 shows the overall structure of the proposed sensorless robust control [28].

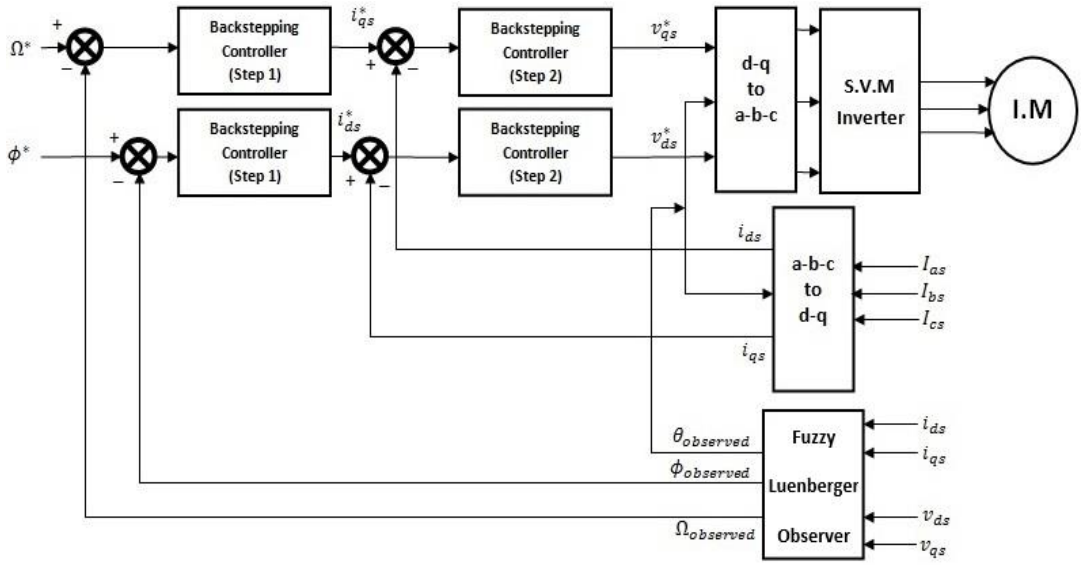

Figure 4. The overall structure of the proposed control

6. RESULTS AND DISCUSSION

To demonstrate the effectiveness of the proposed strategy, the control method and the state observer are implemented in MATLAB/Simulink. The used induction motor rated power and parameters are given in Table 2.

Table 2. Induction motor rated power and parameters

Variable	Symbole	Unit
Rated power	P	3 kW
Stator resistance	R_s	2.20 Ω
Rotor resistance	R_r	2.68 Ω
Stator inductance	L_s	0.229 H
Rotor inductance	L_r	0.229 H
Mutual inductance	L_m	0.217 H
Inertia moment	J	0.047 kg. m^2
Friction coefficient	F_r	0.004 kg. m/s
Poles pair	p	2

6.1. Starting up and steady state with load application

This section presents the starting up state of the induction motor according to speedstep reference of 100 rad/s. Then, a load of 20N.m at t=0.5s is applied and removed at t=0.9s. Figures 5-11 show respectively rotor speed response, rotor speed error, rotor flux, rotor flux error, electromagnetic torque, stator phase current and line voltage.The figures are specified: (a) for PWM-FOC, and (b) for SVM-FOC. The Figures 5-11 show that both techniques prove good dynamic at starting up. We can notice that the speed regulation loop rejects the applied load disturbance quickly. The SVM-FOC in Figure 5(b)kept the same fast speed response of FOC strategy. Since the same backstepping controller is used for both schemes, there is no difference in the transient response.

Then, Figure 9 illustrates the torque responses with load application. It shows that at the beginning the backstepping speed controller operates the system at the physical limit. The PWM-FOC in Figure 10(a) shows a chopped sinusoid waveform of current which indicates the high harmonics level, while SVM-FOC in Figure 10(b) shows a smoother sinusoid waveform. The speed error between the observed and the motor speed does not exceed 3 rad/s in SVM-FOC while it exceeds that in PWM-FOC. The speed response shows a fast and accurate tracking of the imposed high-speed trajectory with minimal steady state error and rise time. Finally, Figure 11shows the comparison of inverter live voltage for both techniques. For the PWM-FOC, it is observed that the voltage amplitude is higher than SVM-FOC, and this can increase the commutation losses.

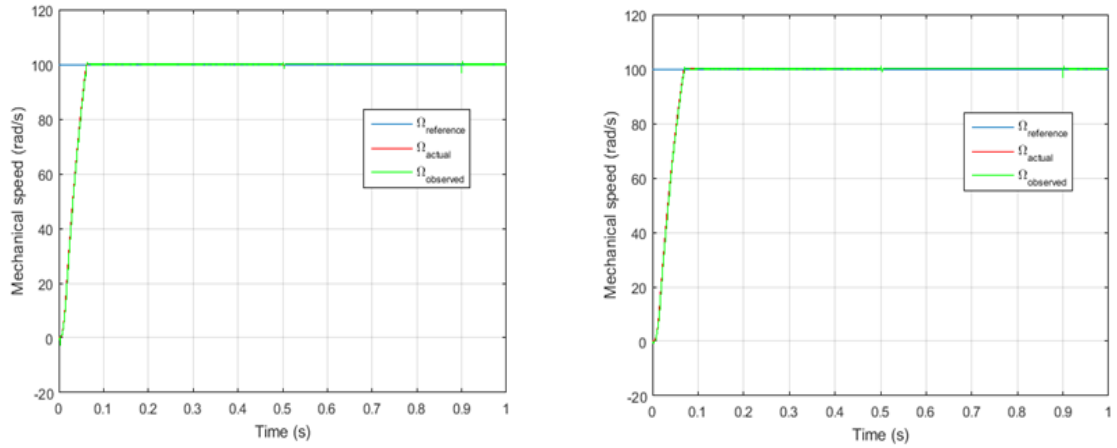

(a) (b)

Figure 5. Rotor speed response

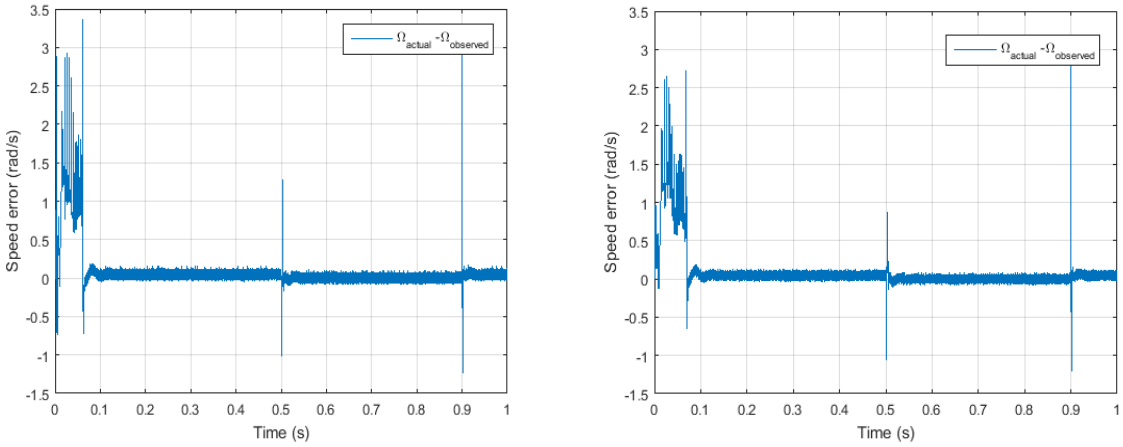

(a) (b)

Figure 6. Rotor speed error

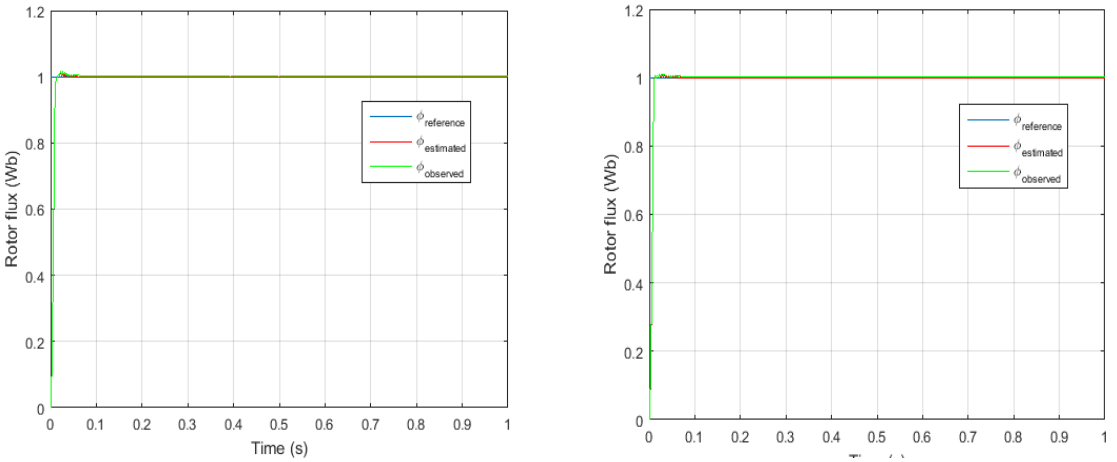

(a) (b)

Figure 7. Rotor flux

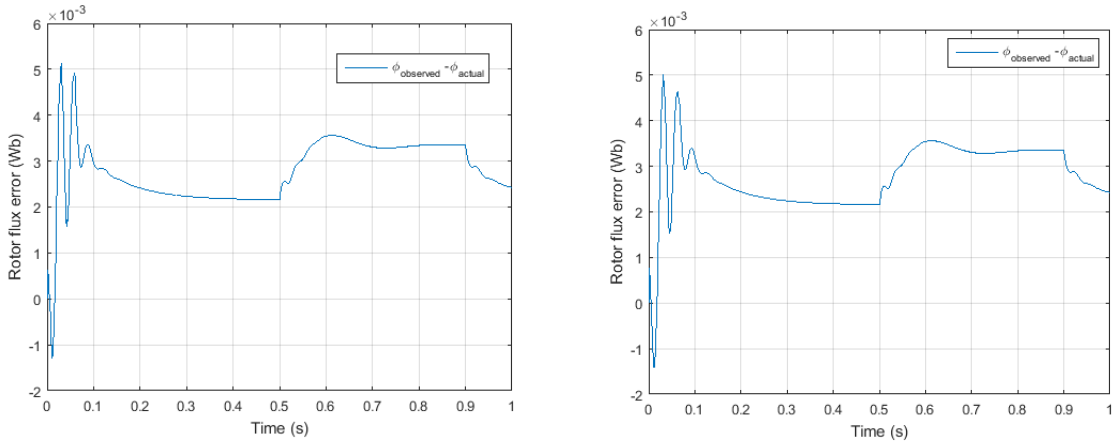

(a) (b)

Figure 8. Rotor flux error

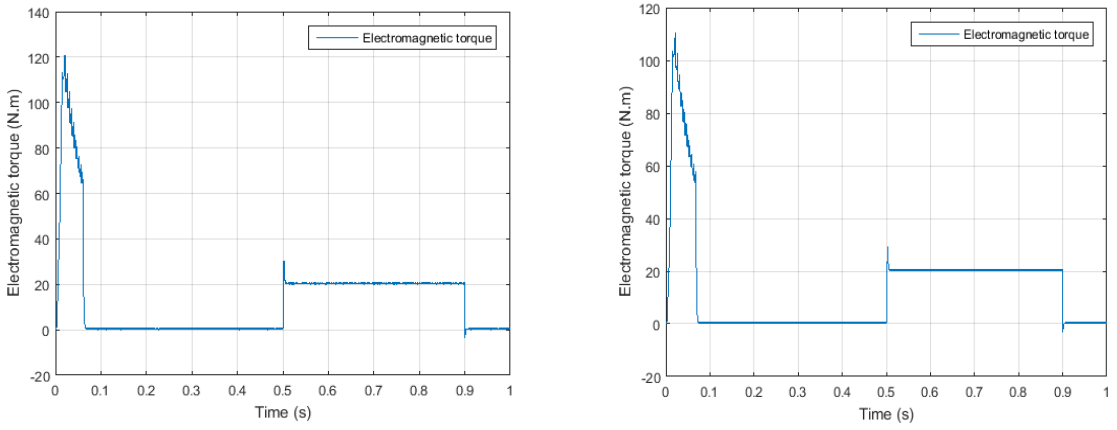

(a) (b)

Figure 9. Electromagnetic torque

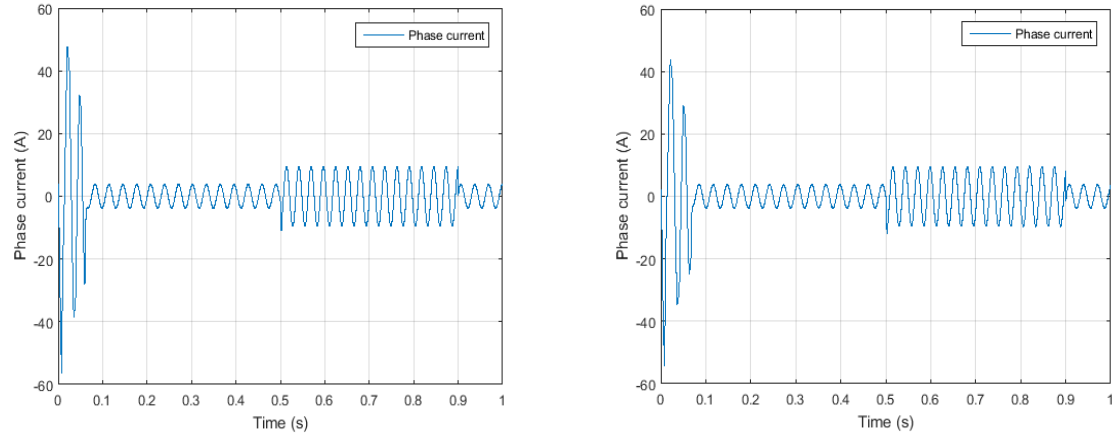

(a) (b)

Figure 10. Stator phase current

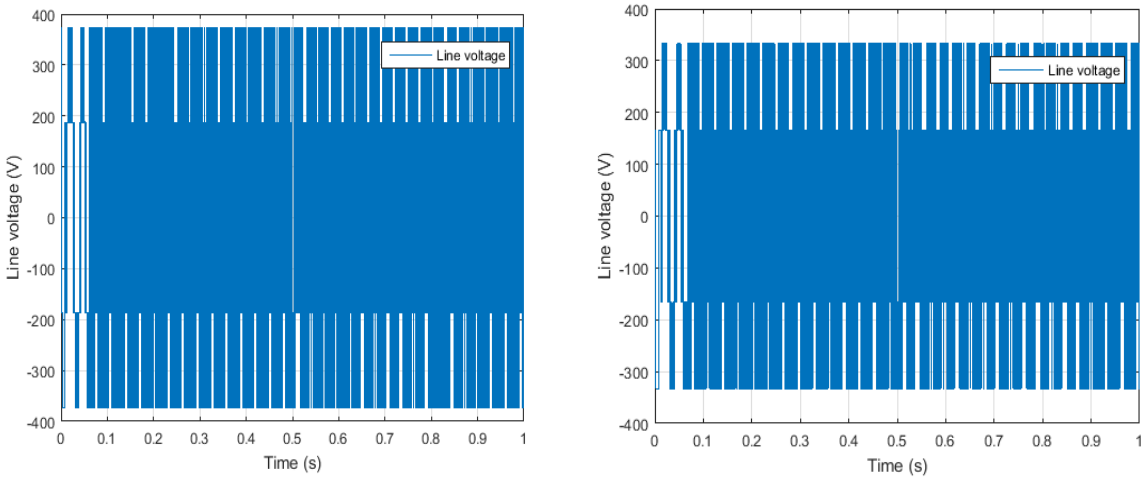

(a) (b)

Figure 11. Line voltage

6.2. THD improvement

This section presents the THD analysis for the electromagnetic torque, the stator phase current and the line voltage. The figures are specified: (a) for PWM-FOC, and (b) for SVM-FOC. The torque THD is reduced from 64.21% to 54.03%, the phase current THD is reduced from 30.94% to 17.87% and the line voltage THD is reduced from 75.63% to 65.54%. The switching frequency of the SVM-FOC technique is constant, the reason is that each inverter's interrupter has a rest moment (switching off) which can reduce the commutation losses even in steady state or in transient operation. Figure 12 shows electromagnetic torque THD. Figure 13 shows phase current THD. Figure 14 shows line voltage THD.

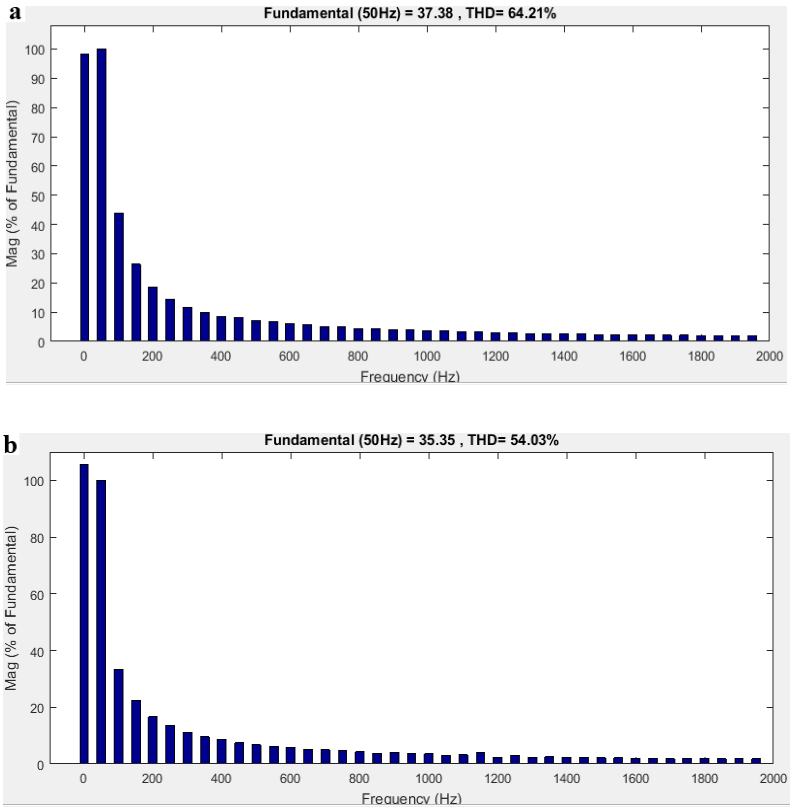

Figure 12. Electromagnetictorque THD

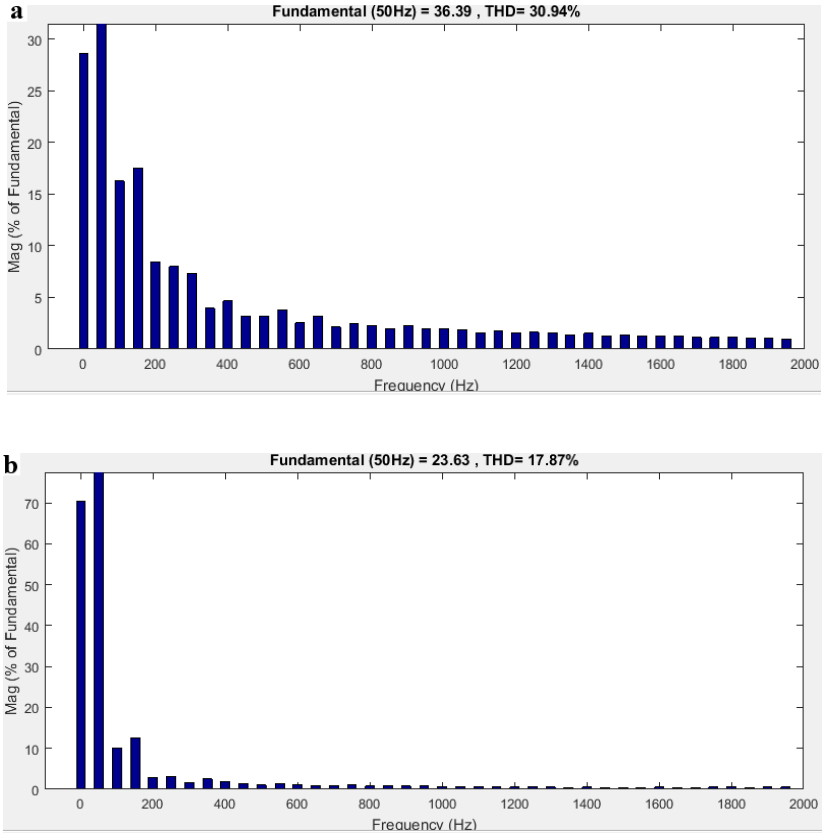

Figure 13. Phase current THD

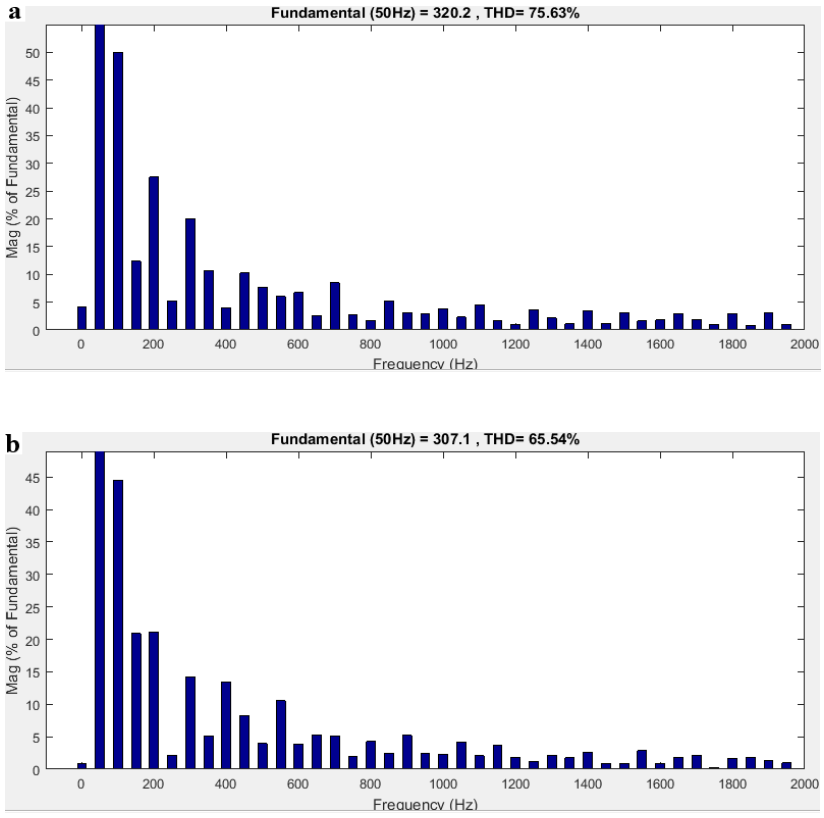

Figure 14. Line voltage THD

7. CONCLUSION

A SVM-FOC for a three-phase induction motor drive is simulated in MATLAB/Simulink, and the dynamic performance is studied too. The starting current, speed regulation, flux distortion and torque pulsation are much lower with SVM technique. The simulated responses show that the system performance during instant load is good, the simulated torque, current and voltage THD during the steady state are improved, with faster dynamic characteristic. In conclusion, SVM-FOC technique has proved good performance dynamic for induction motor vector control type.

ACKNOWLEDGEMENTS

The authors would like to thank the managers and the members of the "Laboratoired'électronique de puissance et commande (EPC) de l'EcoleMohammadiad'Ingénieurs (EMI)" for their precious remarks and suggestions.

REFERENCES

[1] B. Wu and M.,"Narimani, High-power converters and AC drives," John Wiley & Sons, vol. 59, 2017.
[2] R. Singh, S. K. Bajpai, and H. S. Sandhu, "Comparative Study of PWM Control and PI Control of Induction Motor," *Bulletin of Electrical Engineering and Informatics (BEEI)*, vol. 4, no. 1, pp. 53-58, 2015.
[3] G. Kohlrusz and D. Fodor, "Comparison of scalar and vector control strategies of induction motors," *Hungarian Journal of Industry and Chemistry*, vol. 39, no. 2, pp. 265-270, 2011.
[4] K. Hasse, "On the dynamics of speed control of a static ac drive with a squirrel-cage induction machine," PhD, TH Darmstadt, 1969.
[5] F. Blaschke, "The principle of field orientation as applied to the new transvector closed-loop system for rotating-field machines," *Siemens review*, vol. 34, no. 3, pp. 217-220, 1972.
[6] K. A. Chinmaya and G. K. Singh, "Experimental analysis of various space vector pulse width modulation (SVPWM) techniques for dual three-phase induction motor drive," *International Transactions on Electrical Energy Systems*, vol. 29, no. 1, p. e2678, 2019.
[7] P. J. Patel, V. Patel, and P. N. Tekwani, "Pulse-based dead-time compensation method for self-balancing space vector pulse width-modulated scheme used in a three-level inverter-fed induction motor drive," *IET power electronics*, vol. 4, no. 6, pp. 624-631, 2011.
[8] V. Utkin, J. Guldner, and J. Shi, "Sliding mode control in electromechanical systems," CRC press, 2009.
[9] M. Horch, A. Boumediene, and L. Baghli, "Nonlinear Integral Backstepping Control for Induction Motor drive with Adaptive Speed Observer using Super Twisting Strategy," *Electrotehnica, Electronica, Automatica*, vol. 64, no. 1, 2016.
[10] J. Holtz, "Sensorless control of induction motor drives," *Proceedings of the IEEE*, vol. 90, no. 8, pp. 1359-1394, 2002.
[11] P. Vas, "Sensorless vector and direct torque control," Oxford Univ. Press, 1998.
[12] G. Kron, "Generalized theory of electrical machinery," *Transactions of the American Institute of Electrical Engineers*, vol. 49, no. 2, pp. 666-683, 1930.
[13] N. Kiran, "Indirect vector control of three phase induction motor using PSIM," *Bulletin of Electrical Engineering and Informatics (BEEI)*, vol. 3, no. 1, pp. 15-24, 2014.
[14] Y. Zahraoui, A. Bennassar, M. Akherraz and A. Essalmi, "Indirect vector control of induction motor using an extended Kalman observer and fuzzy logic controllers," *2015 3rd International Renewable and Sustainable Energy Conference (IRSEC)*, Marrakech, pp. 1-6, 2015.
[15] H. R. Khoei and E. F. Shahraki, "Fuzzy logic based direct power control of induction motor drive," *Bulletin of Electrical Engineering and Informatics (BEEI)*, vol. 5, no. 3, pp. 296-306, 2016.
[16] A. Zaafouri, C. B. Regaya, H. B. Azza, and A. Chari, "DSP-based adaptive backstepping using the tracking errors for high-performance sensorless speed control of induction motor drive," *ISA transactions*, vol. 60, pp. 333-347, 2016.
[17] B. Aichi, M. Bourahla, and K. Kendouci, "High-Performance Speed Control of Induction Motor Using a Variable Gains Backstepping: Experimental Validation," *International Review of Electrical Engineering (IREE)*, vol. 13, no. 4, pp. 342-351, 2018.
[18] J. Yu, Y. Ma, H. Yu, and C. Lin, "Adaptive fuzzy dynamic surface control for induction motors with iron losses in electric vehicle drive systems via backstepping," *Information Sciences*, vol. 376, pp. 172-189, 2017.
[19] S. A. Vaezi, H. Iman-Eini and R. Razi, "A New Space Vector Modulation Technique for Reducing Switching Losses in Induction Motor DTC-SVM Scheme," *2019 10th International Power Electronics, Drive Systems and Technologies Conference (PEDSTC)*, Shiraz, Iran, pp. 184-188, 2019.
[20] M. Tamilvani, K. Nithya, M. Srinivasan, and S. U. Prabha, "*Harmonic reduction in variable frequency drives using active power filter*,"*Bulletin of Electrical Engineering and Informatics (BEEI)*, vol. 3, no. 2, pp. 119-126,2014.
[21] V. Hari and G. Narayanan, "Space-vector-based hybrid pulse width modulation technique to reduce line current distortion in induction motor drives," *IET Power electronics*, vol. 5, no. 8, pp. 1463-1471, 2012.

[22] Z. Zhang, R. Tang, B. Bai and D. Xie, "Novel Direct Torque Control Based on Space Vector Modulation With Adaptive Stator Flux Observer for Induction Motors," in *IEEE Transactions on Magnetics*, vol. 46, no. 8, pp. 3133-3136, Aug. 2010.
[23] Y. Zahraoui, M. Akherraz, and C. Fahassa, "Induction Motor DTC Performance ImprovementBy Reducing Torque Ripples in Low Speed," *U.P.B. Sci. Bull., Series C,*, vol. 81, no. 3, pp. 249-260, 2019.
[24] F. D. JL, "Machine model based Speed Estimation Schemes for Speed Encoderless Induction Motor Drives: A Survey," *Bulletin of Electrical Engineering and Informatics (BEEI)*, vol. 4, no. 1, pp. 7-17, 2015.
[25] H. R. Khoei and M. Zolfaghari, "New Model Reference Adaptive System Speed Observer for Field-Oriented Control Induction Motor Drives Using Neural Networks," *Bulletin of Electrical Engineering and Informatics (BEEI)*, vol. 5, no. 1, pp. 25-36, 2016.
[26] M. Bahloul, L. Chrifi-Alaoui, S. Drid, M. Souissi, and M. Chaabane, "Robust sensorless vector control of an induction machine using Multiobjective Adaptive Fuzzy Luenberger Observer," *ISA transactions*, vol. 74, pp. 144-154, 2018.
[27] B. Tahar, B. Bousmaha, B. Ismail, and B. Houcine, "Speed Sensorless Field-Oriented Control of Induction Motor with Fuzzy Luenberger Observer," *Electrotehnica, Electronica, Automatica*, vol. 66, no. 4, p. 22, 2018.
[28] Y. Zahraoui, C. Fahassa, M. Akherraz and A. Bennassar, "Sensorless vector control of induction motor using an EKF and SVPWM algorithm," *2016 5th International Conference on Multimedia Computing and Systems (ICMCS)*, Marrakech, pp. 588-593, 2016.

BIOGRAPHIES OF AUTHORS

Yassine Zahraoui,he was born in Casablanca (Morocco), on September 1986. He received the Master's degree in data processing from Hassan 2 University of Casablanca (Morocco) in 2011. Currently he is a PhD student in electrical engineering in laboratory of power electronics and control (PEC) from Mohamed 5 University, Mohammadia School of Engineering. His research interests concern power electronics, AC drives robust control, observation techniques and ripples rejection techniques. E-mail: zahraoui.yassin@gmail.com

Mohamed Akherraz,he graduated from the Mohammadia School of Engineering in Rabat (Morocco). He graduated a Fulbright scholarship to pursue his post-graduate studies. He received his PhD in 1987 from UW, Seattle. He joined the Electrical Engineering Department of the Mohammadia School of Engineering, Rabat where he is currently a Professor of Power Electronics and Electric Drives. His areas of interests are power electronics, electric drives, computer modelling of power electronics circuit and systems drives. E-mail: akherraz@emi.ac.ma

ChaymaeFahassa,she was born in Ksar El-Kebir (Morocco), on September 1987. She received her degree in mechatronics from AbdelmalekEssaadi University of Tetouan in 2012. Currently she is a PhD student in electrical engineering in laboratory of power electronics and control (PEC) from Mohamed 5 University, Mohammadia School of Engineering. Her research interests concern induction motor control using artificial intelligence, sensorless control techniques, hybrid control strategies, power electronics, artificial intelligence and renewable energy. E-mail: fahassa.chaymae@gmail.com

Sara Elbadaoui,she was born in Casablanca (Morocco), on 27 September 1986. She received the Master's degree in automatic, signal processing and industrial computing from Hassan 1 University of Settat (Morocco) in 2012.Currently she is a PhD student in electrical engineering in laboratory of power electronics and control (PEC) from Mohamed 5 University, Mohammadia School of Engineering. Her research interest concern control of the self-excited induction generator. E-mail: elbadaouisara@gmail.com